Spontaneous shape reconfigurations in multicompartmental microcylinders

Kyung Jin Lee[a,1], Jaewon Yoon[b,1], Sahar Rahmani[c], Sangyeul Hwang[a], Srijanani Bhaskar[b], Samir Mitragotri[d], and Joerg Lahann[a,b,c,e,2]

[a]Department of Chemical Engineering, University of Michigan, Ann Arbor, MI 48109; [b]Macromolecular Science and Engineering,University of Michigan, Ann Arbor, MI 48109; [c]Biomedical Engineering, University of Michigan, Ann Arbor, MI 48109; [d]Department of Chemical Engineering, University of California, Santa Barbara, CA 93106; and [e]Materials Science and Engineering, University of Michigan, Ann Arbor, MI 48109

Edited by Robert Langer, Massachusetts Institute of Technology, Cambridge, MA, and approved August 30, 2012 (received for review August 8, 2012)

Nature's particles, such as spores, viruses or cells, are adaptive—i.e., they can rapidly alter major phenomenological attributes such as shape, size, or curvature in response to environmental changes. Prominent examples include the hydration-mediated opening of ice plant seeds, actuation of pine cones, or the ingenious snapping mechanism of predatory Venus flytraps that rely on concave-to-convex reconfigurations. In contrast, experimental realization of reconfigurable synthetic microparticles has been extremely challenging and only very few examples have been reported so far. Here, we demonstrate a generic approach towards dynamically reconfigurable microparticles that explores unique anisotropic particle architectures, rather than direct synthesis of sophisticated materials such as shape-memory polymers. Solely enabled by their architecture, multicompartmental microcylinders made of conventional polymers underwent active reconfiguration including shape-shifting, reversible switching, or three-way toggling. Once microcylinders with appropriate multicompartmental architectures were prepared by electrohydrodynamic cojetting, simple exposure to an external stimulus, such as ultrasound or an appropriate solvent, gives rise to interfacial stresses that ultimately cause reversible topographical reconfiguration. The broad versatility of the electrohydrodynamic cojetting process with respect to materials selection and processing suggests strategies for a wide range of dynamically reconfigurable adaptive materials including those with prospective applications for sensors, reprogrammable microactuators, or targeted drug delivery.

biomimetic | stimuli-responsive | switchable materials | smart materials | electrojetting

The precise engineering of particle properties is important for many biomedical applications including self-assembly, drug delivery, and medical diagnostics (1–7). Beyond particle chemistry, physical properties such as size (2, 8) or shape (9, 10) have been identified as key attributes that govern particle fate in a number of biomedical and biotechnological applications (2). In an attempt to mimic the complexity of biological particles, a number of increasingly sophisticated, multifunctional particles have been devised (11–15). However, with few exceptions (9, 16), these particles lack the ability to undergo spontaneous reconfiguration in response to environmental stimuli (such as pH, salt content, temperature, or redox reactions). In contrast, one of the essential success criteria of living organisms has been the evolution of processes for actuating organ movement (17). This is equally true for bacteria, animals, and plants (18–20). In plants, for instance, organ actuation is often not achieved by metabolically driven processes, but through exploitation of hierarchical geometrical architectures with critical functional feature sizes at the micron and nanometer scale (20). Examples of shape reconfiguration without metabolic activity include the hydration-mediated opening of pine cones (21) and ice plant seeds (22), or the catapult mechanism in fern spores (20). In these cases, changes in the humidity level induce interfacial stresses that result in defined mechanical reconfigurations, such as opening of a spore capsule. A particularly sophisticated adaptive system can be found in Venus flytraps, where the snap-bucking instabilities that lead to millisecond closure of the trapping organ have been linked to convex–concave reconfigurations in the organ wall (23). While these and other adaptive material systems have been hallmarks of nature, they have not yet been systematically realized in synthetic colloidal materials. Synthetic analogues of nature's particles are needed that can spontaneously and reversibly adapt characteristic properties, such as shape, size, or curvature in response to defined external stimuli (19, 24–28). In this paper, we report irreversible as well as reversible reconfiguration of microcylinders with unique anisotropic architectures.

Results and Discussion

Design of Multicompartmenal Microcylinders. Compartmentalized microcylinders are prepared by a scalable process that involves electrohydrodynamic cojetting (29) of two or more polymer solutions followed by microsectioning (30). Fig. 1 *A–C* illustrate the preparation of poly(lactic-co-glycolic acid) (PLGA) microcylinders using electrohydrodynamic cojetting and subsequent microsectioning. As shown in Fig. 1*D*, large populations of microcylinders with close-to-identical diameters and well-defined and controllable length were obtained. Moreover, microcylinders with multiple and variable compartments were prepared using a range of different nozzle configurations including core/shell (31, 32) and dual-core/shell arrangements (Fig. 1*A*). If a PLGA shell stream was employed during electrohydrodynamic cojetting, simultaneous processing of substantially dissimilar materials was possible and allowed for a broad diversification of the compartment compositions. Subsequent removal of the sacrificial shell resulted in microcylinders with substantially different compositions in the individual compartments. In addition, EHD cojetting can provide access to distinct and stable colloidal microcylinders with diameters ranging from hundreds of nanometers to hundreds of micrometers (see *SI Appendix*, Fig. S1 for PLGA cylinders with submicron diameters).

Selected target structures and their potential reconfigurability are shown in Fig. 1*E*. Depending on the composition selected for the individual microcompartments, these microcylinders can undergo programmable shape-shifting of individual compartments or entire particles (Fig. 1). When the microcylinders are comprised of polymer compartments with distinct swellability, reversible two-way shape-switching is observed in response to changes in the solvent environment. Fully reversible three-way shape-toggling

Author contributions: S.M. and J.L. designed research; K.J.L., J.Y., S.R., S.H., and S.B. performed research; K.J.L., J.Y., S.M., and J.L. analyzed data; and K.J.L., J.Y., and J.L. wrote the paper.

The authors declare no conflict of interest.

This article is a PNAS Direct Submission.

[1]K.J.L. and J.Y. contributed equally to this work.

[2]To whom correspondence should be addressed. E-mail: lahann@umich.edu.

This article contains supporting information online at www.pnas.org/lookup/suppl/doi:10.1073/pnas.1213669109/-/DCSupplemental.

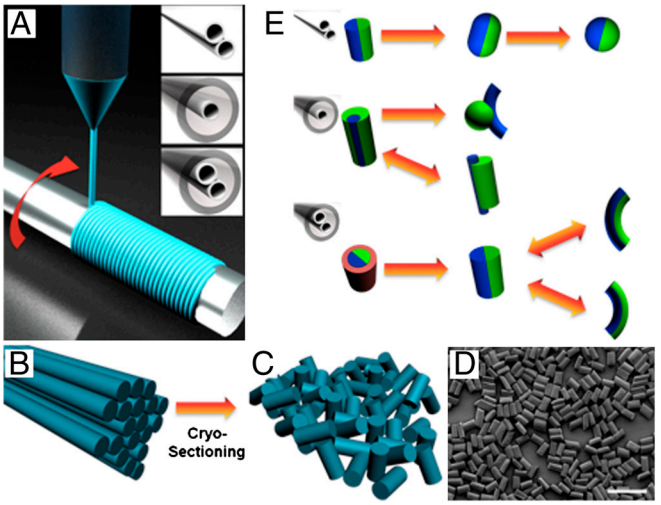

Fig. 1. Diagram of the electrohydrodynamic (EHD) cojetting and microsectioning process that leads to multicompartmenal microcylinders. (*A–C*) Well-aligned PLGA fibers were obtained using a rotating wheel collector, and the fiber bundles were then converted into microcylinders through microsectioning. Specific needle configurations are illustrated in the inset of the figure (*A*). (*D*) Scanning electron microscopy (SEM) image of typical PLGA microcylinders (sectioned at a length of 30 μm, scale bar: 100 μm). (*E*) Overview of three types of shape reconfiguration based on multicompartmental microcylinders: (*i*) shape-shifting, (*ii*) reversible switching, and (*iii*) three-way toggling.

occurs in bicompartmental microcylinders, if one compartment is composed of a hydrogel and the other of an organogel.

On-Demand Shape-Shifting. We initially focused on shape-shifting of multicompartmental microcylinders into spheres. For polymer particles, the thermodynamically most favorable state is that of a sphere and most particle fabrication methods have resulted in spherical polymer particles so far. Thus, particle engineers have been accustomed to almost exclusively dealing with spherical polymer particles. Recent exceptions include the synthesis of certain inherently nonspherical polymer particles (9, 33–36), energy-driven conversion of spherical particles into shaped particles via stretching at elevated temperatures (37–39), and the electrohydrodynamic cojetting procedure used herein to create microcylinders (30).

If multicompartmental microcylinders are comprised of polymers below their glass transition temperature, their shapes are arrested in the cylindrical shape and the particles remain stable over extended times (Fig. 2*A*). Here PLGA was used, because it is biodegradable, has a glass temperature (T_g) of 47–48 °C, and a relatively low surface tension (The water/air contact angle of a film casted from the PLGA used in this study was 92°). Fig. 2*B* shows a population of PLGA-based microcylinders, which was stored below the glass transition temperature of the polymer for three days ($T_g > T_P$ regimen, where T_g = glass transition temperature and T_P = polymer temperature). To induce shape-shifting, one can either increase T_P or lower T_g (39). Ultrasound treatment for two minutes in water converted the microcylinders completely and homogenously into spheres (Fig. 2*C*). The choice of ultrasound as the stimulus for shape reconfiguration has a number of advantages; it can be applied remotely and has already been broadly used in medical and nondestructive imaging (40).

If the microcylinders were treated with ultrasound in an ice bath, the localized heating effect of the ultrasound was suppressed and shape-shifting into spheres was no longer observed (Fig. 2*D*). In this case, the particles remained in the $T_g > T_P$ regimen and their initial cylindrical shapes were maintained, albeit there was a rounding of the edges of the microcylinders (Fig. 2*E*). Ultrasound-mediated cavitations as well as other mechanical effects were ruled out as the driving force for shape-shifting,

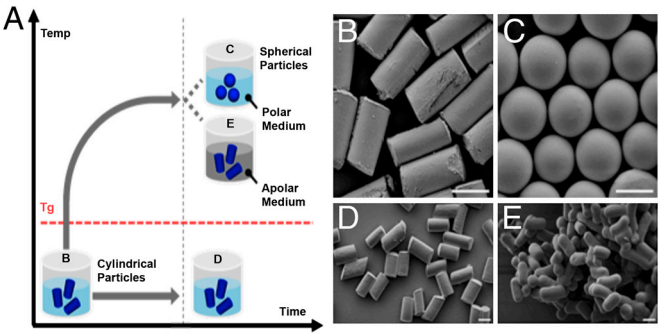

Fig. 2. Reconfiguration of polymeric microcylinders into microspheres. (*A*) A graphical representation of temperature versus time relations for the shape-shifting process. When polymeric microcylinders are treated with ultrasound, the increase in temperature above the T_g of the polymer causes cylindrical particles (*B*) to take on a spherical envelope (*C*). As control experiments, the microcylinders were treated with ultrasound in an ice bath (*D*), and in heptane (bp = 98 °C) (*E*). The ice bath is used for keeping the temperature below T_g of polymer during sonication, and heptane is used as an apolar medium, which does not favor reconfiguration of the microcylinders into spheres. Scale bars are all 20 μm.

because they should be approximately temperature-independent (41). For a particle above its glass transition temperature, shape-shifting is favored by higher free surface energy of the particle surface and lower polymer viscosity (37). Assuming a close-to-constant polymer viscosity, the driving force for particle reconfiguration should be dominated by minimization of the free surface energy. The shape-shifting thus depends on the surface tension of the solvent, in which the reconfiguration is carried out. To confirm this hypothesis, we suspended PLGA microcylinders in either apolar heptane ($\varepsilon = 1.9$) or polar water ($\varepsilon = 80$). After treatment with ultrasound for 2 min, particles underwent shape-shifting in water, but not in heptane. This finding confirms that minimization of free surface energy of the polymer particles plays a dominating factor for particle reconfiguration (Fig. 2*E*).

Once this shifting mechanism was confirmed and procedures for quantitative shifting were established, we assessed whether shape-shifting can be extended to microcylinders with multiple

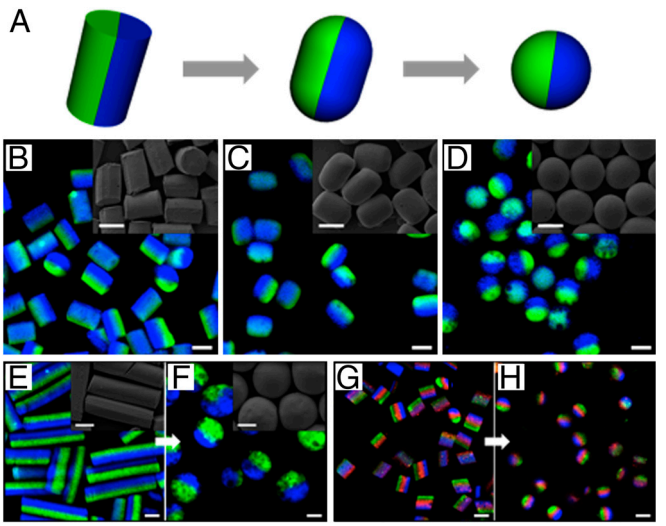

Fig. 3. Isotropic shape-shifting of microcylinders into microspheres. (*A*) A schematic representation of the shape-shifting of bicompartmental particles by ultrasound. (*B–D*) Corresponding CLSM and SEM (*inset*) images of bicompartmental microcylinders (30 μm in length) before and after (*Left* to *Right*, *C* indicates an intermediate state) shape-shifting. (*E*, *F*) Reconfiguration of bicompartmental microcylinders (70 μm in length) before (*Left*) and after (*Right*) shape-shifting. (*G*, *H*) Reconfiguration of tricompartmental microcylinders before (*Left*) and after (*Right*) shape-shifting (scale bar: 20 μm).

distinct compartments (Fig. 3*A*). Specifically, PLGA microcylinders with an average aspect ratio of 1.48±0.10 and two equally sized compartments were prepared and exposed to ultrasound for 3 min (Fig. 3 *B–D*). The average diameter after shape-shifting was 26.85±0.88 μm as compared to an average diameter of 20.06±0.56 μm for the microcylinders prior to shape-shifting. The mean aspect ratio of the microcylinders changed from 1.48±0.10 to 1.05±0.03, which is indicative of nearly perfect spheres. In addition, confocal laser scanning microscopy (CLSM) analysis after shape-shifting confirmed maintenance of well-defined, bicompartmental particle architectures. To further demonstrate the generality of the shape-shifting approach, we prepared bicompartmental microcylinders with an average diameter and length of 20.69±0.69 μm and 70.00±0.88 μm (Fig. 3*E*). Subsequent shape-shifting resulted in microspheres with diameters of 37.17±1.22 μm and aspect ratios of 1.02±0.01 (Fig. 3*F*). Again, the bicompartmental architecture of the particles was fully maintained. Beyond bicompartmental architectures, one may expect a higher propensity for inhomogeneities during shape-shifting, as the number of compartments increases or the size of individual compartments decreases. Developing a thorough understanding of these subtle limitations of the shape-shifting process may become increasingly important, as recent work suggests that microcylinders with as many as seven compartments can be experimentally created (30). We thus prepared two types of tricompartmental microcylinders: those with sequential (Fig. 3*G*) and pie-shaped compartmentalization (*SI Appendix*, Fig. S2*A*). As shown in Fig. 3*H* and *SI Appendix*, Fig. S2*B*, CLSM analysis of the compartmentalized particles confirmed that the original compartmentalization patterns were fully maintained after shape-shifting. Similarly, heptacompartmental particles can be prepared by shape-shifting of corresponding microcylinders. Interestingly, the direct synthesis of heptacompartmental microspheres via electrospraying has so far not been realized, which elevates the fact that the procedure reported here can be used to create a broad range of compartmentalized microspheres (*SI Appendix*, Fig. S2 *C* and *D*).

Particle Fabrication via Partial Shape-Shifting. In principle, one of the major advantages of using compartmentalized microcylinders for shape-shifting is that appropriate selection of the compartment materials may lead to partial shape-shifting—i.e., only certain compartments of the microcylinders are converted into spherical shapes, while the rest is not switched. Such partial shape

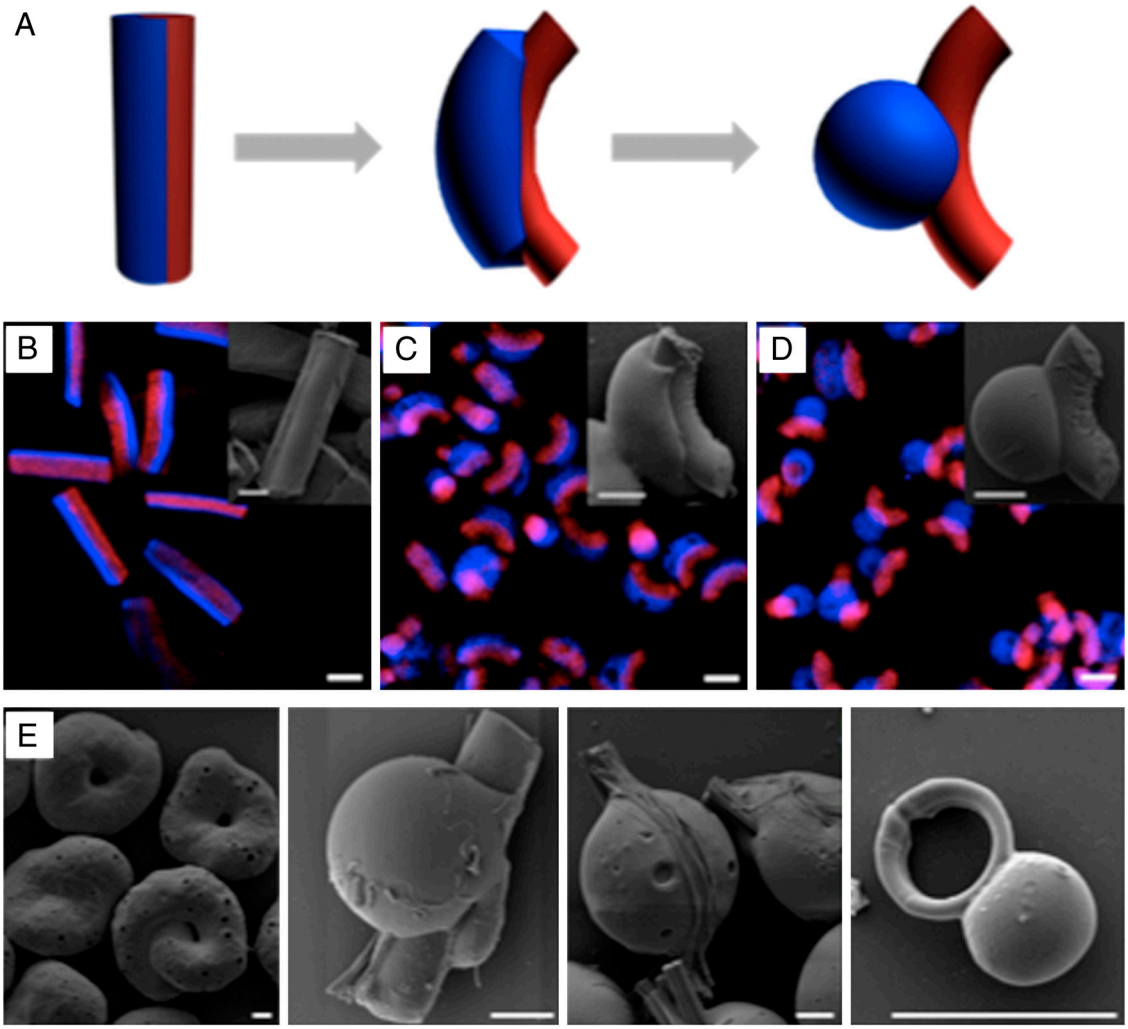

Fig. 4. Anisotropic shape-shifting of multicompartmental microcylinders. (*A*) A schematic illustration of the shape-shifting from *B* to *D*. (*B–D*) CLSM and SEM (*inset*) images of bicompartmental PMMA/PLGA microcylinders before and after (*Left* to *Right*) shape-shifting. The blue and red fluorescent dyes were incorporated in PLGA and PMMA, respectively. Upon ultrasound treatment, only the PLGA compartments were reconfigured into spherical shapes (*C* indicates an intermediate state). Scale bars in CLSM and SEM images are 20 μm and 10 μm, respectively. (*E*) SEM images of various shapes of multicompartmental particles with different polymers that were produced from the similar process. From left to right: Bicompartmenal PLGA/(PLGA+PMMA), PVCi/PLGA microparticles, tricompartmental PLGA/(PLGA+PVCi)/ PLGA microparticles, bicompartmental PS/PLGA microparticles. All scale bars are 10 μm.

reconfiguration can be expected to yield colloidal particles with entirely new shapes. The experimental validation required microcylinders with compartments that feature polymers with distinct T_g, plasticizability or rigidity. Here, poly(methyl methacrylate) (PMMA) and PLGA were used for electrohydrodynamic cojetting, because PMMA has a T_g of 115–116 °C, which is substantially higher than that of PLGA (47–48 °C). Heating the bicompartmental microcylinders to a temperature between the two glass transition temperatures resulted in selective shape-shifting of the PLGA compartment only (Fig. 4 *A–D*). Using this approach, a wide range of particles was realized through programmable reconfiguration of microcylinders with previously unseen shapes. Fig. 4*E* shows four examples of reconfigured polymer particles (corresponding confocal images are provided in *SI Appendix*, Fig. S3). Changes in the aspect ratios of bicompartmental PLGA/PMMA particles yielded "bull-head" or "ring" particles. When the weight percentage of PMMA was decreased from 100% (Fig. 3 *B–D*) to 10% in one compartment (Fig. 4*E*, *Left*), particles underwent increasing bending, which may be attributed to a decreased rigidity of the particles. We further prepared bicompartmental particles with poly(vinyl cinnamate) (PVCi) confined in one compartment. Because PVCi is a photocrosslinkable polymer, exposure to UV light can be used to render the PVCi containing compartments inert to the ultrasound-induced reconfiguration (Fig. 4*E*) (42). The particle shapes observed here closely resembled the theoretically predicted equilibrium shapes (*SI Appendix*, Fig. S4) (43, 44). Specifically, the simulated equilibrium states for bicompartmental PLGA/PLGA (*SI Appendix*, Fig. S4 *A–C*) and PVCi/PLGA microcylinders (*SI Appendix*, Fig. S4 *D–F*) were in excellent agreement with the experimentally observed particle shapes. Similarly, tricompartmental PLGA/(PLGA+PVCi)/PLGA cylinders were reconfigured into particles with centrosymmetric polymer backbones (Fig. 4*E*).

Fully Reversible Particle Switching. While all particles discussed so far underwent one-way reconfiguration—i.e., their shapes were moving towards a thermodynamic equilibrium envelope—multicompartmental microcylinders can also be designed to show fully reversible and controllable two-way shape-switching, as illustrated in Fig. 5 *A* and *D*. In Fig. 5*A*, a PLGA solution was used as the shell stream and a hydrogel [here, 1:1 (w/w) mixture of polyethylene glycol diglycidyl ether and branched polyethyleneimine was used as the hydrogel component] was processed through the core (*SI Appendix*). Fig. 5*B* displays a representative SEM image of bicompartmental Hydrogel/PLGA microcylinders after electrospinning, thermal crosslinking, and microsectioning. The thermal crosslinking was necessary to avoid dissolution of the core polymer in water. The hydrogel core compartment was swollen by 280% in water, while the PLGA compartment maintained its initial shape. The mismatch in mechanical properties caused reversible expansion and retraction of the hydrogel neck upon exposure to water (Fig. 5*C*). Moreover, the synthesis of bicompartmenal microcylinders that featured PVCi and poly(ethylene oxide) (PEO) (Fig. 5*E*) in a side-by-side arrangement led to reversible bending of the microcylinders upon immersion into water (Fig. 5*D* and *SI Appendix*). After crosslinking, the PVCi was swellable in dioxane, whereas the PEO compartment maintained the original shape in dioxane, resulting in reversible bending (Fig. 5*F* and Movie S1). Highly repeatable, reversible reconfiguration was observed under these conditions (*SI Appendix*, Fig. S12*A*) with bending variabilities below 10% (*SI Appendix*, Fig. S12*B*).

Three-Way Toggling of Bicompartmental Microcylinders. Fully reversible shape-toggling can be realized using bicompartmental microcylinders composed of two different stimuli responsive gel compartments (Fig. 6*A* and *SI Appendix*). Experimentally, microcylinders configured as a pair of an organogel (i.e., PVCi) and a hydrogel (i.e., a chemically crosslinked 1:1 mixture of poly(ethylene imine) (PEI)/PEO) compartment were prepared and evaluated for their mechanical actuation upon exposure to either dioxane or water (Fig. 6*B* and Movie S2). In dioxane, the PVCi compartment was selectively swollen, whereas the hydrogel compartment expanded only in water. In the dry state, however, both compartments were contracted and the microcylinders assumed a straight shape. For 200-μm fibers, closed circles were formed by swelling in dioxane (Fig. 6*C*). With longer fibers, helical structures were obtained, where the PVCi compartment was exclusively located in the outside rim of the helix (in Fig. 6*D*, *Top*). Subsequent immersion into water resulted in reconfiguration of the helices into straight fibers (Movie S3). In contrast, the hydrogel compartments were selectively swollen at pH 4 resulting again in a helical configuration (bottom-most in Fig. 6*D* and *SI Appendix*). The actuation angle of the bicompartmental microcylinders successively varied with the solvent ratio of dioxane and water leading to a continuous transition from concave to convex (Fig. 6*E*). The herein observed curvature reconfigurations of synthetic microparticles closely mimic the concave-to-convex transitions observed in Venus flytraps (23).

With these fully reversible shape-switching microcylinders, a broad range of biomimetic motion, for instance, actuation of pine cones (21) and ice plant seeds (22), or the catapult mechanism in fern spores can be mimicked. As a representative example of these applications, we demonstrate reversible grabbing and releasing motion of artificial soft-actuators using bicompartmental microfibers (Fig. 7). Fig. 7*A* displays reversible shape-toggling behavior of a bicompartmental PVCi/Hydrogel microfiber segment in water and dioxane. The selective swelling and deswelling

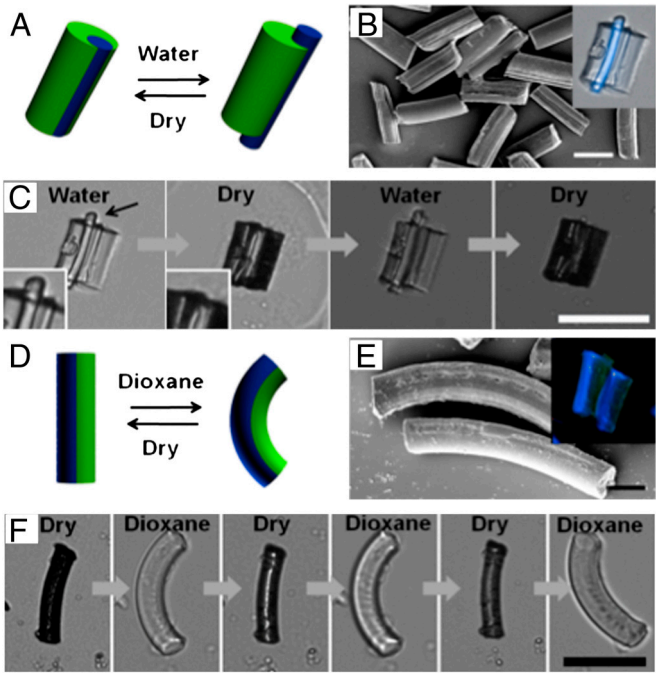

Fig. 5. Two-way shape-switching of bicompartmental microcylinders. (*A*) Schematic illustration of two-way shape-switching of Hydrogel/PLGA core/shell microcylinders by swelling–deswelling of the core compartment upon environmental stimuli (from water to dry state). (*B*) SEM and fluorescence optical microscopy (OM) (*inset*) images of Hydrogel/PLGA microcylinders with a length of 50 μm (scale bar: 25 μm). OM images are obtained in the presence of water, and thus the core compartment is selectively swollen by water. (*C*) OM images of the swelling and deswelling actions of the core compartments that expand reversibly in water (scale bar: 50 μm). (*D*) Schematic illustration of the reversible bending caused by the swelling–deswelling of one compartment only. (*E*) SEM and CLSM (*inset*) images of PVCi/PEO bicompartmental microcylinders (scale bar: 10 μm). (*F*) OM images of the selective swelling of PVCi in the presence of dioxane, resulting in reversible actuation (scale bar: 50 μm).

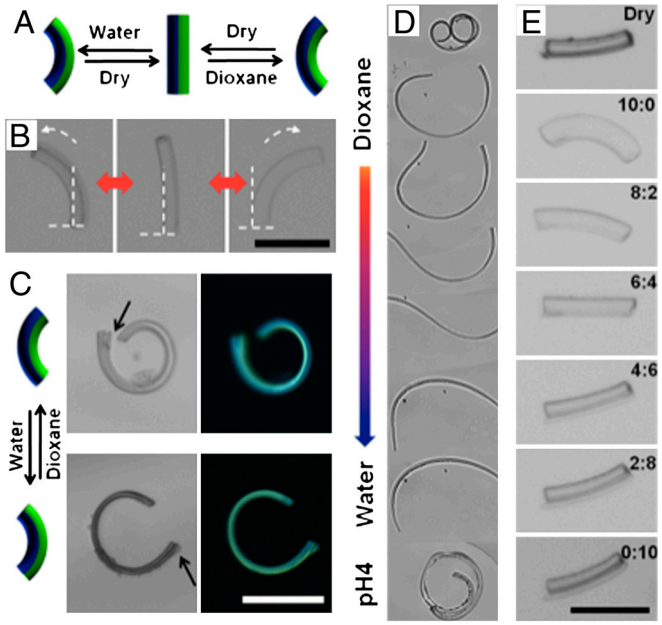

Fig. 6. Three-way shape-toggling of bicompartmental microcylinders. (*A*) Schematic diagram of microcylinders that are comprised of compartments containing a hydrogel and an organogel. (*B*) OM images of bicompartmental PVCi/Hydrogel microcylinders (sectioned at a length of 50 μm) showing the full range of actuation, as the solvent environment changes from 100% water to 100% dioxane (*Left*: in water, *Center*: dry state, and *Right*: in dioxane; scale bar: 50 μm). (*C*) OM (*Left*) and fluorescence OM (*Right*) images of 200-μm microcylinders showing shape-toggling behavior (scale bar: 100 μm). (*D*) The actuation behavior of a 0.7-mm-long fiber (*SI Appendix*). (*E*) OM images of the actuation angles controlled by adjusting the ratios of dioxane and water. The ratios indicate dioxane and water, respectively (scale bar: 50 μm).

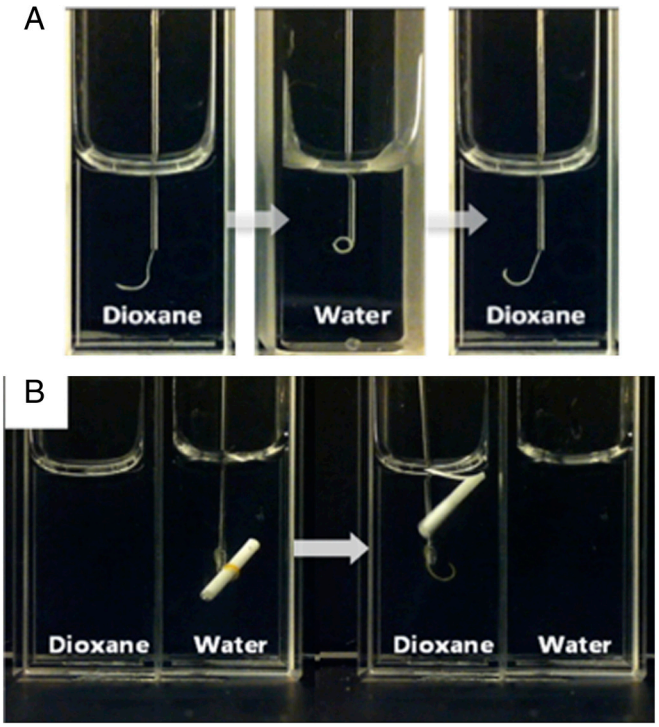

Fig. 7. Grabbing motion of PVCi/Hydrogel microfibers. (*A*) photographs displaying shape-toggling of a micromanipulator based on bicompartmental PVCi/Hydrogel microfiber segments. (*B*) Reversible grabbing and release motion of the compartmentalized micromanipulator [grabbing an object by actuation in water and releasing it in dioxane; for comparison, a conventional quartz fluorescence cell (1 cm × 1 cm) has been used]. These images are captured from Movie S4.

of each compartment leads to reversible grabbing motion, similar to that of an Octopus arms, which may be applied in soft-robotics (45, 46). Fig. 7*B* in combination with Movie S4 unambiguously demonstrate grabbing and release motion of a simple micromanipulator devised from the bicompartmental PVCi/Hydrogel microfiber segment shown in Fig. 7*A*.

Conclusions

In summary, multicompartmental microcylinders with appropriately designed compartments can undergo defined shape reconfiguration, such as toggling, bending, or shape-shifting. An interesting aspect of these multicompartmental microcylinders is that compartments can be made of different polymers, which selectively respond to a specific stimulus. If multicompartmental microcylinders are exposed to ultrasound as the external stimulus, irreversible one-way shape-shifting can lead to reconfiguration into near perfect spheres. Two-way reversible shape transitions require multicompartmental microcylinders that are comprised of stimulus-responsive as well as inert compartments. If the compartments of the microcylinders are however composed of a hydrogel and an organogel, the individual compartments display different swelling responses. This can give rise to fully reversible three-way shape-toggling with well-defined convex-to-concave transitions. The controlled reconfiguration of multicompartmental microcylinders constitutes an important step towards the biomimetic development of adaptive materials with potential applications as sensors, actuators, or switchable drug delivery carriers.

Materials and Methods

PLGA Microcylinders. The experimental setup contained a syringe pump (Fisher Scientific Inc., USA), a power supply (DC voltage source, Gamma High Voltage Research, USA), and a rotary collector (Synthecon Inc., modified to experimental requirements). The PLGA solutions were delivered at a constant flow rate of 0.05 ml/h via a vertically positioned syringe equipped with 23 G needle (Nordson EFD, USA). A driving voltage of 11 kV resulted in a stable jet and fiber bundles were collected at a tip-to-ground distance of 5 cm (30). In case where compositionally dissimilar compartments were needed, PLGA was employed as a shell stream. See the *SI Appendix* for detailed needle arrangements and preparation procedures for different types of multicompartmental microfibers (*SI Appendix*, Table S1). Microsectioning of the fiber bundles was done using a cryostat microtome (Microm HM550, Thermo Fisher Scientific Inc., Germany). The samples were embedded into a sectioning medium (Tissue-Tek O.C.T. Compound, Andwin Scientific, USA), cooled to −20 °C, and microsectioned at a desired length. Preparation methods for different multicompartmental microcylinders are listed in *SI Appendix*, Table S1. In all cases, PVCi and a hydrogel [PEG diglycidyl ether+branched PEI (1:1, w/w)] underwent photo and thermal crosslinking, respectively, prior to microsectioning. When microcylinders were produced by dual-core shell jetting, the PLGA shell compartment was removed and bicompartmental microcylinders having PVCi/PEO and PVCi/Hydrogel were obtained.

Shape-Reconfiguring of Microcylinders. The typical shape-shifting procedure of PLGA microcylinders involved dispersion of approximately 10,000 cylinders in 1 mL of medium in Eppendorf tube and treatement with ultrasound (Ultrasonic Processor, Cole-Parmer, USA) at room temperature. The medium used for the ultrasound treatment was either 2 v/v% Tween 20/DI water or a mixture of ethanol and 2 v/v% Tween 20/DI water (1:1, v/v). The detailed experimental conditions for each shape-shifting process of multicompartmental microcylinders are listed in *SI Appendix*, Table S2. Reversible actuation behavior of bicompartmental microcylinders was observed by introducing either water or dioxane. Specifically, bicompartmental Hydrogel/PLGA and PVCi/PEO microcylinders show reversible two-way shape-switching upon water and dioxane, respectively. Three-way shape-toggling of bicompartmental PVCi/Hydrogel microcylinders was induced by adjusting the ratio between dioxane and water.

ACKNOWLEDGMENTS. The authors thank the American Cancer Society (RSG–08–284–01–CDD) for financial support and acknowledge funding from the Multidisciplinary University Research Initiative of the Department of Defense and the Army Research Office (W911NF-10–1–0518). The authors would like

to thank the Microscopy and Image Analysis Lab (MIL) at the University of Michigan for use of the CLSM, SEM, and cryostat microtome, and the Department of Chemistry at the University of Michigan for use of the differential scanning calorimetry (DSC) equipment.

1. Langer R, Tirrell DA (2004) Designing materials for biology and medicine. *Nature* 428:487–492.
2. Mitragotri S, Lahann J (2009) Physical approaches to biomaterial design. *Nat Mater* 8:15–23.
3. Petros RA, DeSimone JM (2010) Strategies in the design of nanoparticles for therapeutic applications. *Nat Rev Drug Discov* 9:615–627.
4. Kaehr B, Shear JB (2008) Multiphoton fabrication of chemically responsive protein hydrogels for microactuation. *Proc Natl Acad Sci USA* 105:8850–8854.
5. Yoo JW, Irvine DJ, Discher DE, Mitragotri S (2011) Bio-inspired, bioengineered, and biomimetic drug delivery carriers. *Nat Rev* 10:521–535.
6. Sacanna S, Pine DJ (2011) Shape-anisotropic colloids: Building blocks for complex assemblies. *Curr Opin Colloid Interface Sci* 16:76–105.
7. Yoon J, Lee KJ, Lahann J (2011) Multifunctional polymer particles with distinct compartments. *J Mater Chem* 21:8502–8510.
8. Kohane DS (2007) Microparticles and nanoparticles for drug delivery. *Biotechnol Bioeng* 96:203–209.
9. Merkel TJ, et al. (2011) Using mechanobiological mimicry of red blood cells to extend circulation times of hydrogel microparticles. *Proc Natl Acad Sci USA* 108:586–591.
10. Decuzzi P, Ferrari M (2008) The receptor-mediated endocytosis of nonspherical particles. *Biophys J* 94:3790–3797.
11. Chen Q, Bae SC, Granick S (2011) Directed self-assembly of a colloidal kagome lattice. *Nature* 469:381–384.
12. Yoshida M, Lahann J (2008) Smart nanomaterials. *ACS Nano* 2:1101–1107.
13. Stuart MAC, et al. (2010) Emerging applications of stimuli-responsive polymer materials. *Nat Mater* 9:101–113.
14. Lv S, et al. (2010) Designed biomaterials to mimic the mechanical properties of muscles. *Nature* 465:69–73.
15. Oh JK, Drumright R, Siegwart DJ, Matyjaszewski K (2008) The development of microgels/nanogels for drug delivery applications. *Prog Polym Sci* 33:448–477.
16. Yoo JW, Mitragotri S (2010) Polymer particles that switch shape in response to a stimulus. *Proc Natl Acad Sci USA* 107:11205–11210.
17. Fratzl P, Elbaum R, Bungert I (2008) Cellulose fibrils direct plant organ movements. *Faraday Discuss* 139:275–282.
18. Young KD (2006) The selective value of bacterial shape. *Microbiol Mol Biol Rev* 70:660–703.
19. Huebsch N, Mooney DJ (2009) Inspiration and application in the evolution of biomaterials. *Nature* 462:426–432.
20. Bungert I, Fratzl P (2009) Actuation systems in plants as prototypes for bioinspired devices. *Phil Trans R Soc A* 367:1541–1557.
21. Dawson C, Vincent JFV, Rocca AM (1997) How pine cones open. *Nature* 390:668–668.
22. Harrington MJ, et al. (2011) Origami-like unfolding of hydro-actuated ice plant seed capsules. *Nat Commun* 2:1–7.
23. Forterre Y, Skotheim JM, Dumais J, Mahadevan L (2005) How the Venus flytrap snaps. *Nature* 433:421–425.
24. McConney ME, Anderson KD, Brott LL, Naik RR, Tsukruk VV (2009) Bioinspired material approaches to sensing. *Adv Mater* 19:2527–2544.
25. Yoshida R (2010) Self-oscillating gels driven by the Belousov-Zhabotinsky reaction as novel smart materials. *Adv Mater* 22:3463–3483.
26. Huck WTS (2008) Responsive polymers for nanoscale actuations. *Mater Today* 11:24–32.
27. Sidorenko A, Krupenkin T, Taylor S, Fratzl P, Aizenberg J (2007) Reversible switching of hydrogel-actuated nanostructures into complex micropatterns. *Science* 315:487–490.
28. Ohm C, et al. (2011) Microfluidic synthesis of highly shape-anisotropic particles from liquid crystalline elastomers with defined director field configuration. *J Am Chem Soc* 133:5305–5311.
29. Bhaskar S, Lahann J (2009) Microstructured materials based on multicompartmental fibers. *J Am Chem Soc* 131:6650–6651.
30. Bhaskar S, Hitt J, Chang SWL, Lahann J (2009) Multicompartmental microcylinders. *Angew Chem Int Ed* 48:4589–4593.
31. Yu JH, Fridrikh SV, Rutledge GC (2004) Production of submicrometer diameter fibers by two-fluid electrospinning. *Adv Mater* 16:1562–1566.
32. Greiner A, Wendorff JH (2007) Electrospinning: A fascinating method for the preparation of ultrathin fibers. *Angew Chem Int Ed* 46:5670–5703.
33. Dendukuri D, Pregibon DC, Collins J, Hatton TA, Doyle PS (2006) Continuous-flow lithography for high-throughput microparticle synthesis. *Nat Mater* 5:365–369.
34. Sacanna S, Rossi L, Pine DJ (2012) Magnetic click colloidal assembly. *J Am Chem Soc* 134:6112–6115.
35. Shum HC, Zhao Y-j, Kim S-H, Weitz DA (2011) Multicompartment polymersomes from double emulsions. *Angew Chem Int Ed* 50:1648–1651.
36. Forster JD, et al. (2011) Assembly of optical-scale dumbbells into dense photonic crystals. *ACS Nano* 5:6695–6700.
37. Champion JA, Katare YK, Mitragotri S (2007) Making polymeric micro-and nanoparticles of complex shapes. *Proc Natl Acad Sci USA* 104:11901–11904.
38. Ho CC, Keller A, Odell JA, Ottewill RH (1993) Preparation of monodisperse ellipsoidal polystyrene particles. *Colloid Polym Sci* 271:469–479.
39. Sung KE, et al. (2008) Programmable fluidic production of microparticles with configurable anisotropy. *J Am Chem Soc* 130:1335–1340.
40. Ferrara KW, Borden MA, Zhang H (2009) Lipid-shelled vehicles: Engineering for ultrasound molecular imaging and drug delivery. *Acc Chem Res* 42:881–892.
41. Caruso MM, et al. (2009) Mechanically-induced chemical changes in polymeric materials. *Chem Rev* 109:5755–5798.
42. Lee KJ, et al. (2011) Compartmentalized photoreactions within compositionally anisotropic Janus microstructures. *Macromol Rapid Commun* 32:431–437.
43. Brakke KA (1992) The surface evolver. *Exp Math* 1:141–165.
44. Cho YS, et al. (2007) Particles with coordinated patches or windows from oil-in-water emulsions. *Chem Mater* 19:3183–3193.
45. Ilievski F, Mazzeo AD, Shepherd RF, Chen X, Whitesides GM (2011) Soft robotics for chemists. *Angew Chem Int Ed* 50:1890–1895.
46. Calisti M, et al. (2011) An octopus-bioinspired solution to movement and manipulation for soft robots. *Bioinspir Biomim* 6:036002.